FxpNet: Training a Deep Convolutional Neural Network in Fixed-Point Representation

Xi Chen*, Xiaolin Hu
Tsinghua National Laboratory for
Information Science and Technology (TNList)
Department of Computer Science and Technology
Tsinghua University, Beijing 100084, China
aaron.xichen@gmail.com
xlhu@tsinghua.edu.cn

Hucheng Zhou, Ningyi Xu
Microsoft Research Asia
Beijing 100084, China
{huzho, ningyixu}@microsoft.com

***Abstract*—We introduce FxpNet, a framework to train deep convolutional neural networks with low bit-width arithmetics in both forward pass and backward pass. During training FxpNet further reduces the bit-width of stored parameters (also known as primal parameters) by adaptively updating their fixed-point formats. These primal parameters are usually represented in the full resolution of floating-point values in previous binarized and quantized neural networks. In FxpNet, during forward pass fixed-point primal weights and activations are first binarized before computation, while in backward pass all gradients are represented as low resolution fixed-point values and then accumulated to corresponding fixed-point primal parameters. To have highly efficient implementations in FPGAs, ASICs and other dedicated devices, FxpNet introduces Integer Batch Normalization (IBN) and Fixed-point ADAM (FxpADAM) methods to further reduce the required floating-point operations, which will save considerable power and chip area. The evaluation on CIFAR-10 dataset indicates the effectiveness that FxpNet with 12-bit primal parameters and 12-bit gradients achieves comparable prediction accuracy with state-of-the-art binarized and quantized neural networks.**

I. Introduction

In recent years, advances in deep Convolutional Neural Networks (CNNs) have changed the landscape of many non-trival Artificial Intelligence tasks, such as computer vision [1], [2], natural language processing [3], [4] and speech recognition [5], [6]. CNNs usually contain large amounts of learnable parameters and most of them take days or weeks to train on one or more fast and power-hungry GPUs [7]–[10]. There have been substantial research efforts [9]–[11] made on speeding up offline training and online serving, especially in power-efficient devices such FPGAs and dedicated ASICs [12]–[17]. Among all these methods, model quantization [9]–[11], [18], [19] has been considered the most promising approach, which has not only significantly accelerated the speed and increased power-efficiency, but also achieved comparable accuracy. Model quantization tries to quantize the model parameters (as well as activations and gradients) to low bit-width values, while model binarization [20]–[25] further pushes the limit of quantization by extremely quantizing the parameter as one single bit (-1 and 1). As a consequence, during inference, memory footprint and memory accesses can be drastically reduced, and most arithmetic operations can be implemented with bit-wise operations, i.e., binary convolution kernel [22].

However, all these state-of-the-art methods neglect the quantization of `primal` parameters, which is defined as those high resolution weights and biases stored to be updated across different training mini-batches. These `primal` parameters will be quantized or binarized before every forward pass, and the associated gradient accumulations are still performed in the floating-point domain. Thus, the FPGA and ASIC still need to implement expensive floating-point multiplication-accumulation to handle parameter updates, and even the much more expensive nonlinear quantization arithmetics.

In this paper, we present FxpNet which pushes the limit of quantization and binarization by representing the `primal` parameters in a fixed-point format, which has never been considered before in binarized networks to the best of our knowledge. This brings advantages in two ways: 1) It decreases the bit-width of `primal` parameters which dramatically reduces the total memory footprint. For example, an 8-bit fixed-point representation can reduce the total memory footprint by $4\times$ compared with the floating-point counterpart. This makes it possible to place the parameters in on-chip memory rather than off-chip memory on dedicated hardware devices like FPGAs and ASICs, which means 100x energy efficiency of memory accessing with 45nm CMOS technology [10]. 2). Low bit-width of fixed-point arithmetic operations in FPGAs and ASICs are much more faster and energy efficient than floating-point ones [16]. Besides, fixed-point operators will generally dramatically reduce logic usage and power consumption, combined with higher clock frequency, shorter pipelines, and increased throughput capabilities. Combining these advantages with binarized inference, it is possible to make highly efficient computing devices that are flexible enough to train themselves in a new and continously changing environment with a limited power budget.

This paper makes the following contributions:

- We introduce FxpNet to train a binarized neural network,

*This work was done when Xi Chen was an intern at MSRA

978-1-5090-6182-2/17/$31.00 ©2017 IEEE

whose `primal` parameters and gradients are represented as adaptive fixed-point values. In forward pass, both fixed-point `primal` weights and activations are binarized before computation. In backward pass gradients are also quantized to low resolution fixed-point values and then accumulated to the corresponding fixed-point `primal` parameters. In this way, bit convolution kernels [22] can be used in FxpNet to accelerate both training and inference.
- To have highly efficient implementation in FPGAs and dedicated ASICs, FxpNet further adopts linear rather than non-linear quantization to save on the quantization cost, and utilizes Integer Batch Normalization (IBN) and Fixed-point ADAM (FxpADAM) methods to further reduce the required floating-point operations.
- The evaluation on the CIFAR-10 dataset indicates the effectiveness that FxpNet with 12-bit `primal` parameters and 12-bit gradients achieves a similar accuracy to the state-of-art BNN [22] with the float (32-bit) counterparts.

II. FxpNet

In this section we first introduce vanilla BNN, which is derived from popular BNNs [22], [25]. The intention is to design a concise BNN which serves as a starting point and baseline of FxpNet by taking both computation efficiency and prediction accuracy into consideration. We then describe the fixed-point representation as well as critical techniques in FxpNet, and give a detailed description of the training algorithm.

A. Vanilla BNN

As indicated by [20], [22], [23], [25], binarizing weight and activation can significantly speedup the performance by the bit convolution kernels. There are two binarization approaches, deterministic and stochastic, used to transform floating-point value into one single bit. Stochastic binarization could get slightly better performance [25] at the cost of more complex implementation since it requires hardware to generate random bits when quantizing. Thus, we propose using only the deterministic binarization method (a simple sign function):

$$w^b = \mathrm{sign}(w) = \begin{cases} +1 & w \geq 0, \\ -1 & otherwise. \end{cases} \tag{1}$$

Binarization dramatically reduces computation and memory consumption in forward pass, nevertheless, the derivative of the sign function is 0 almost everywhere, makes the gradients of the cost c can't be propagated in backward pass. To address this problem, we adopt the "straight-through estimator" (STE) method [5], [27], and use the same STE formulation in [22]:

$$\begin{aligned} \textbf{Forward}: & \; r_o = \mathrm{sign}(r_i) \\ \textbf{Backward}: & \; \frac{\partial c}{\partial r_i} = \frac{\partial c}{\partial r_o} \mathbf{1}_{|r_i| \leq 1} \end{aligned} \tag{2}$$

Above STE preserves gradient information and cancels the gradient when r_i is too large. No-cancelling will cause a significant performance drop. As also pointed out in QNN [25], STE can also be seen as applying the well-known *hard tanh* activation function to r_i, defined as

$$HT(r_i) = \begin{cases} +1 & r_i > 1, \\ r_i & r_i \in [-1, 1], \\ -1 & r_i < -1. \end{cases} \tag{3}$$

Correspondingly, the derivative of *hard tanh* is defined as

$$\frac{\partial HT(r_i)}{\partial r_i} = \begin{cases} 0 & r_i > 1, \\ 1 & r_i \in [-1, 1], \\ 0 & r_i < -1. \end{cases} \tag{4}$$

which is exactly the STE defined in Equation 2. With Equation 2 and 4, BNN binarizes both activations and weights during forward pass, while still reserving real-valued gradients of weights to guarantee that Stochastic Gradient Descent (SGD) works well. BNN further proposes shift-based Batch Normalization (BN) and a shift-based ADAM learning rule to accelerate training and reduce the impact of weights' scale. The shift operations are intended to replace the expensive multiplications, while here we argue that required log operations are also expensive. So we reserve the floating point version of BN and ADAM as the baseline. A detailed description of our baseline BNN can be found in Section III.

B. Fixed-Point Format

FxpNet maintains primal weights and gradients as fixed-point numbers. Different from floating point format which has a sign, an exponent and a mantissa, the fixed-point format consists of a l-bit signed integer mantissa and a global scaling factor (e.g. $2^{-\mathrm{n}}$) shared among all fixed-point values, i.e.,

$$\mathbf{v} = \begin{pmatrix} v_1 \\ \vdots \\ v_K \end{pmatrix} = \begin{pmatrix} m_1 \\ \vdots \\ m_K \end{pmatrix} \cdot 2^{-\mathrm{n}} \tag{5}$$

where $m_1, \cdots, m_K, \mathrm{n} \in \mathbb{Z}$. Here the integer n actually indicates the radix point position of the l-bit fixed-point number. We use the following conversion formulation to quantize a floating-point value x into a l-bit fixed-point value with the scaling factor $2^{-\mathrm{n}}$:

$$\mathrm{FXP}(x, l, n) = \mathrm{Clip}(\lfloor \frac{x}{2^{-n}} + 0.5 \rfloor \cdot 2^{-n}, \mathrm{MIN}, \mathrm{MAX}) \tag{6}$$

where

$$\begin{cases} \mathrm{MIN} = -2^{l-1} * 2^{-n} \\ \mathrm{MAX} = (2^{l-1} - 1) * 2^{-n} \end{cases} \tag{7}$$

Note that 1) Equation 6 defines both the saturating behavior and rounding to nearest behavior (ties are rounded to positive infinity); 2) The MIN and MAX values are defined according to the range of l-bit integer in two's complement, which fully utilize all ordinality 2^l and make addition/subtraction circuits simple.

C. Quantization with Adaptive Fixed-point Scheme

It is well known that the magnitudes of weight, activation and gradient will fluctuate during the whole training procedure. We demonstrate these characteristics with our results in Figure 1, where $conv11$, $conv12$ and $conv31$ are three different layers of a 5-layer floating point CNN on CIFAR-10 dataset (see Session III). It can be observed that gradients

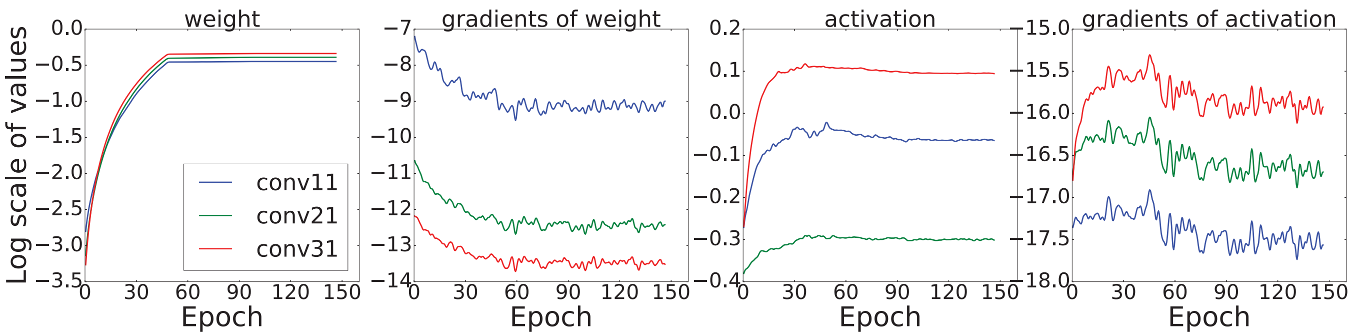

Fig. 1. $\mathrm{Mean}(\mathrm{Abs}(\cdot))$ of weights, activations and corresponding gradients in $\log 2$ scale

for both activation and weight diminish slowly, and weights and activations boost rapidly at the beginning and converge with tiny changes.

In order to capture the change of parameters and gradients and fit their actual value distribution, it is necessary to assign different bit-widths and scaling factors to different groups of variables in different layers. FxpNet utilizes the dynamic fixed-point transformation [28] with adaptive update of scaling factor [18]. Algorithm 1 depicts the details. In particular, differs from $\mathrm{Clip}(\cdot)$ in Equation 6, $\mathrm{OverflowRate}(\cdot)$ from Alrogithm 1 will count the number of values that are not in $[\min, \max]$. Section II-E explores the effectiveness regarding hyper-parameters such as the initial bitwidth, scaling factor, and the overflow threshold.

Algorithm 1 Adaptive update of scaling factor.

Require: matrix $\mathbf{M}$, scaling factor 2^{sf_t}, bitwidth bw, overflow threshold thr
Ensure: $2^{\mathrm{sf}_{t+1}}$
if $\mathrm{OverflowRate}(\mathbf{M}, \mathrm{bw}, \mathrm{sf}_t) \geq \mathrm{thr}$ **then**
  $\mathrm{sf}_{t+1} \leftarrow \mathrm{sf}_t - 1$
else if $\mathrm{OverflowRate}(\mathbf{M}, \mathrm{bw}, \mathrm{sf}_t + 1) < \mathrm{thr}$ **then**
  $\mathrm{sf}_{t+1} \leftarrow \mathrm{sf}_t + 1$
else
  $\mathrm{sf}_{t+1} \leftarrow \mathrm{sf}_t$
end if

Compared with binarized weights and activations, gradients usually need higher precision [18], [24]. Hubara et al. [25] (QNN) point out that linear quantization does not converge well and they instead use a logarithmic method. DoReFa-Net [24] utilizes well-designed and complicated non-linear function to quantize the gradient, which contains costly $\mathrm{division}$ operations. All these non-linear operations will inevitably increase computation overhead, especially on FPGAs. Table I compares the gradient quantization approaches used in existing works, where the area cost of quantization operations is estimated if they are implemented in FPGA.

We choose to adopt linear quantization to trade for simplicity. While simply propagate gradients with the same scaling factor (statically) will introduce too strong regularization and impede convergence (see III-B for details), FxpNet revises the potential accuracy loss by the adaptive scaling factors among layers, as detailed in the following subsections.

TABLE I
QUANTIZATION OPERATIONS OF DIFFERENT METHODS

Method	Quantization operation	LEs[1]	DSPs[1]
DoReFa-Net [24]	division	907	4
QNN [25]	log	1504	4
Miyashita et al. [19]	log	1504	4
FxpNet	linear($\mathrm{l} = 16$)	35	0

[1] Logical Elements (LEs) and Digital Signal Processors (DSPs)

D. Forward Pass

With all the techniques aforementioned, we begin to introduce the framework to train FxpNet. First we give the details of forward pass.

Figure 2 depicts the fixed-point building block (FPB) of CNNs.

- All grey squares represent fixed-point variables, while all black squares are binarized variables.
- W_k^{fxp} and b_k^{fxp} represent the primal weight and bias of layer k, respectively. In FxpNet, they are represented as a fixed-point format rather than floating-point format as in previous works. The primal variables (weights and bias) will be iteratively updated during the whole training procedure.
- In forward pass, primal weights are first binarized (Blue layer), which converts the input to $+1$ or -1 according to sign function (Equation 1). X_k^b represents either input images (for the first block) or output binarized activation of the previous layer. In the former case, X_k^b can be regarded as an 8-bit integer vector (0-255), while in the latter case X_k^b is a binary ($+1$ or -1) vector. In both case Conv operation only contains integer multiplication and accumulation and can be computed by bit convolution kernels [22], [25]. Note that the first layer is processed as the following (in the same way as BNN and QNN):

$$s = x \cdot w^b;$$
$$s = \sum_{n=1}^{8} 2^{n-1}(x^n \cdot w^b). \tag{8}$$

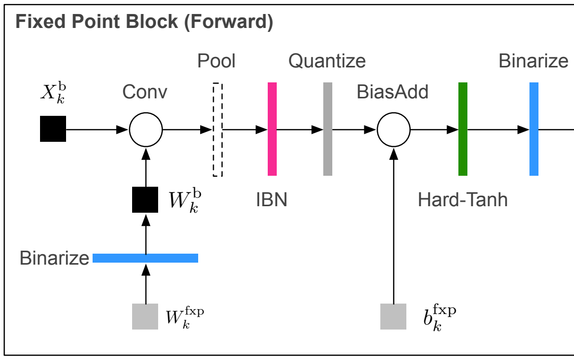

Fig. 2. Forward pass of fixed-point block (FPB).

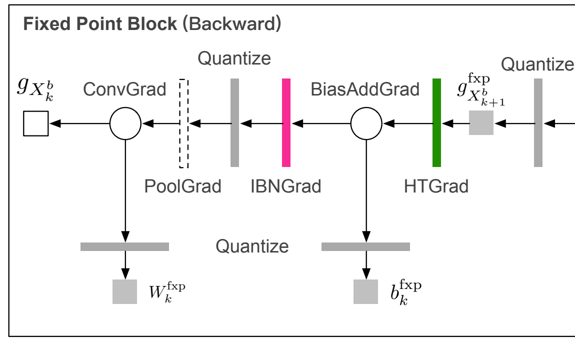

Fig. 3. Backward pass of fixed-point block in FxpNet.

- The pink layer stands for the integer batch normalization (IBN) layer, which normalizes input tensor with mean and variance within a mini-batch. Different from standard BN and shift-based BN [25] which are performed in the floating-point domain, all intermediate results involved in IBN are either 32-bit integers or low resolution fixed-point values. (see Section III-A for more discussion). Algorithm 2 describes the details of IBN.
- The gray layer refers to fixed-point quantization which converts the output of IBN to fixed-point values (see Equation 6)
- The green layer is the non-linear activation function ($\mathrm{Hard\text{-}Tanh}$ shown in Equation 3).
- Besides, we disable the γ and substitute the β in standard BN with an extra bias b in $\mathrm{BiasAdd}$ block.

Algorithm 2 Integer Batch Normalization. $\mathrm{Round}(\cdot)$ refers to rounding to the nearest 32-bit integer operation. $\mathrm{FXP}(\cdot)$ denotes Equation 6 and we omit l and n for simplicity.

Require: Fixed-point values of x over a mini-batch $\mathbb{X}_{\text{in}} = \{x_1, \cdots, x_N\}$
Ensure: Normalized output $\mathbb{X}_{\text{out}} = \{y_1^{\text{fxp}}, \cdots, y_N^{\text{fxp}}\}$

$\mathrm{sum1} \leftarrow \sum_{i=1}^{N} x_i$
$\mathrm{sum2} \leftarrow \sum_{i=1}^{N} x_i^2$
$\mathrm{mean} \leftarrow \mathrm{Round}(\mathrm{sum1}/N)$
$\mathrm{var} \leftarrow \mathrm{Round}(\mathrm{sum2}/N) - \mathrm{mean}^2$
$y_i \leftarrow (x_i - \mathrm{mean})/\mathrm{Round}(\sqrt{\mathrm{var}})$
$y_i^{\text{fxp}} \leftarrow \mathrm{FXP}(y_i)$

For the purpose of reducing computation complexity, pooling layers after FPB (if they exist) will be absorbed into FPB and inserted between the Conv layer and the IBN layer as shown in Figure 2. Note that the last FPB does not contain $\mathrm{Hard\text{-}Tanh}$ and $\mathrm{Binarize}$ layer, i.e., the $\mathrm{SoftmaxCrossEntropyLoss}$ layer is computed in the floating-point domain.

E. Backward Pass

In backward pass, float gradients coming from the last $\mathrm{SoftmaxCrossEntropyLoss}$ layer will be first converted to fixed-point values (denoted as $g_{X_{k+1}^b}^{\text{fxp}}$). The specific backward process is shown in Figure 3 from right to left.

- All white squares represent non-fixed-point values
- Green layer (HTGrad) computes the gradient of $\mathrm{Hard\text{-}Tanh}$ according to Equation 4.
- Gradients that flow into the IBN layer have fixed-point values. Although we can compute IBN in forward pass with fixed-point format, unfortunately, non-negligible accuracy degradation occurs if we restrict the backward computation of IBN ($\mathrm{IBNGrad}$) in fixed-point representation. Consequently, we choose to relax it back to the floating-point domain. We add a quantization layer right after $\mathrm{IBNGrad}$ in order to transform float gradients back to fixed-point format. This quantization layer will be associated with a unique scaling factor that will be adaptively updated according to Algorithm 1.
- $\mathrm{ConvGrad}$ layer further propagates the gradients with respect to X_k^b of last layer and W_k^b. Consider X_k^b as either an 8-bits integer vector (the first layer) or as a binary vector, and W_k^b is binary vector, thus the $\mathrm{ConvGrad}$ operation only contains fixed-point multiplication and accumulation.
- Last but not least, we utilize fixed-point ADAM optimization method (FxpADAM) to apply the fixed-point gradient to fixed-point primal parameters rather than standard ADAM [29]. (See Algorithm 3 for details)

Algorithm 3 Fixed-point ADAM learning rule. g_t^2 denotes element-wise square $g_t \circ g_t$. For simplicity we fix 1-β_1^t and 1-β_2^t to 1-β_1 and 1-β_2 respectively. $\mathrm{FXP}(\cdot)$ denotes Equation 6. Default settings are $1-\beta_1 = 2^{-4}$, $1-\beta_2 = 2^{-8}$ and $\epsilon = 2^{-20}$

Require: Previous primal parameters θ_{t-1} with fixed-point format $l_1.n_1$, their gradients g_t with fixed-point format $l_2.n_2$, learning rate η_t
Ensure: Updated fixed-point primal parameters θ_t

$m_t^{\text{fxp}} \leftarrow \mathrm{FXP}(\beta_1 \cdot m_{t-1} + (1-\beta_1) \cdot g_t, l_2, n_2)$
$v_t^{\text{fxp}} \leftarrow \mathrm{FXP}(\beta_2 \cdot v_{t-1} + (1-\beta_2) \cdot g_t^2, 2l_2, 2n_2)$
$u_t^{\text{fxp}} \leftarrow \mathrm{FXP}(\sqrt{v_t^{\text{fxp}} + \epsilon}, l_2, n_2)$
$\theta_t \leftarrow \mathrm{FXP}(\theta_{t-1} - \eta_t \cdot \sqrt{1-\beta_2}/(1-\beta_1) \cdot m_t^{\text{fxp}}/u_t^{\text{fxp}}, l_1, n_1)$

Algorithm 4 Training a FxpNet. C is the loss function within minibatch and L is the number of layers. $(\circ)$ denotes element-wise mulitiplications and $\mathrm{LRDecay}(\cdot)$ stands for how to decay the learning rate. $\mathrm{FxpADAM}(\cdot)$ means updating parameters with Fixed-point ADAM optimitzation methods. $\mathrm{ClipGrad}(\cdot)$ refers to clamping the absolute values of gradients larger than 1. $\mathrm{Binarize}(\cdot)$ denotes Equation 1 and $\mathrm{HardTanh}(\cdot)$ denotes Equation 3. $\mathrm{FXP}(\cdot)$ denotes Equation 6 and we omit l and n for simplicity.

Require: a minibatch of inputs x_0^b and targets y^*, previous weights W_t^{fxp}, b_t^{fxp} and learning rate η_t in iteration t,
Ensure: updated W_{t+1}^{fxp}, b_{t+1}^{fxp} and η_{t+1}

{1.Computing the parameter gradients:}
{1.1. Forward propagation:}
for $k \leftarrow 0, L-1$ **do**
  $W_{k,t}^b \leftarrow \mathrm{Binarize}(W_{k,t}^{\mathrm{fxp}})$
  $s_k \leftarrow \mathrm{BiasAdd}(\mathrm{FXP}(\mathrm{IBN}(\mathrm{Conv}(x_k^b, W_{k,t}^b))), b_{k,t}^{\mathrm{fxp}})$
  if $k < L-1$ **then**
    $x_k \leftarrow \mathrm{HardTanh}(s_k)$
    $x_{k+1}^b \leftarrow \mathrm{Binarize}(x_k)$
  else
    $x_{k+1} \leftarrow s_k$
  end if
end for
{1.2. Backward propagation:}
Compute $g_{x_L} \leftarrow \frac{\partial C}{\partial x_L}$ given x_L and y^*
for $k \leftarrow L-1, 0$ **do**
  $g_{x_{k+1}^b}^{\mathrm{fxp}} \leftarrow \mathrm{FXP}(g_{x_{k+1}^b})$
  if $k < L-1$ **then**
    $g_{s_k}^{\mathrm{fxp}} \leftarrow g_{x_{k+1}^b}^{\mathrm{fxp}} \circ \mathbf{1}_{|x_{k+1}| \le 1}$
  else
    $g_{s_k}^{\mathrm{fxp}} \leftarrow g_{x_{k+1}^b}^{\mathrm{fxp}}$
  end if
  $g_{x_k^b} \leftarrow \mathrm{BackwardInput}(g_{s_k}^{\mathrm{fxp}}, W_{k,t}^b)$
  $g_{W_{k,t}^{\mathrm{fxp}}} \leftarrow \mathrm{BackwardWeight}(g_{s_k}^{\mathrm{fxp}}, x_k^b)$
  $g_{b_{k,t}^{\mathrm{fxp}}} \leftarrow \mathrm{BackwardBias}(g_{s_k}^{\mathrm{fxp}})$
end for
{2. Accumulating the parameters gradients}
for $k \leftarrow 0, L-1$ **do**
  $W_{k,t+1}^{\mathrm{fxp}} \leftarrow \mathrm{Clip}(\mathrm{FxpADAM}(W_{k,t}^{\mathrm{fxp}}, g_{W_{k,t}^{\mathrm{fxp}}}, \eta_t))$
  $b_{k,t+1}^{\mathrm{fxp}} \leftarrow \mathrm{FxpADAM}(b_{k,t}^{\mathrm{fxp}}, g_{b_{k,t}^{\mathrm{fxp}}}, \eta_t)$
  $\eta_{t+1} \leftarrow \mathrm{LRDecay}(\eta_t, t)$
end for

F. Overall Algorithm

Combining all ingredients, we describe the whole training algorithm of FxpNet in Algorithm 4.

III. Experiments

In this section, we evaluate the important factors of FxpNet that affect the final prediction accuracy, including the batch normalization scheme, bit-width of primal parameters and bit-width of gradients. We independently investigate the effect of each component by applying them one by one on vanilla BNN respectively. Finally, we combine all these components to obtain FxpNet and explore the extremity of bit-width while maintaining prediction accuracy.

TABLE II
Model complexity

Model	#Parameter	#MACs
Model-S	0.58M	39.82M
Model-M	2.32M	156.60M
Model-L	9.29M	623.74M
BNN [22], QNN [25]	14.02M	616.97M
Miyashita et al. [19]	14.02M	616.97M

Evaluation setup. We use CIFAR-10 [30] for evaluation that is an image classification benchmark with 60K 32×32 RGB tiny images. It consists of 10 classes of object, including airplane, automobile, bird, cat, deer, dog, frog, horse, ship and truck. Each class has 5K training images and 1K test images. To evaluate model fitting capability and training efficiency, we have designed three networks with different sizes by stacking multiple FPB, including Model-S (Small), Model-M (Medium) and Model-L (Large). The overall network structure is illustrated in Figure 4. All convolution kernels are 3×3, and the number of output channels in the first convolution layer is 32, 64 and 128 for Model-S, Model-M and Model-L, respectively. Table II lists the number of parameters and the number of multiply-accumulate operations (MACs) in these three models. "$\times 2$ (4 or 8)" in in C21 in Figure 4 means the number of output channels in C21 is two times (4X or 8X) as much as the number in C11 and C12. It is noteworthy that the loss layer is computed in the floating-point domain in both forward pass (Figure 4a) and backward pass (Figure 4b).

In all experiments we train 37,500 iterations with mini-batch size of 200, i.e., given with 50K training images, there are a total of 150 epochs and each epoch has 250 iterations. We use either FxpADAM or the standard ADAM optimization method [29] with initial learning of 2^{-6} and we decrease learning by a factor of 2^{-4} every 50 epochs. Dropout [31] has not been used.

A. Effects of Batch Normalization Scheme

We evaluate the effects of different batch normalization schemes on prediction accuracy, including standard floating-point BN and different bit-width of IBN output. Here we keep primal parameters and all gradients in floating-point format, and we use the standard ADAM algorithm to optimize the network. Note that we perform Algorithm 1 upon the bit-width of IBN output every 1,125 iterations (3% of total iterations), and the threshold of Algorithm 1 is set to 0.01%.

As shown in Figure 5, the network is robust to the loss of resolution within IBN output, as low as 6-bit.

B. Effects of Primal Parameters Bit-width

To evaluate the effects resulting from bit-width of primal parameters (weights and bias), we conduct experiments with floating-point gradients. As show in Figure 6, 8-bits primal

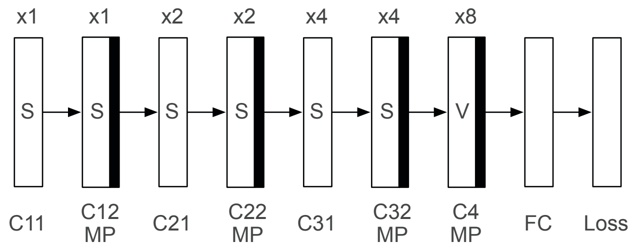

(a) Forward pass of whole network

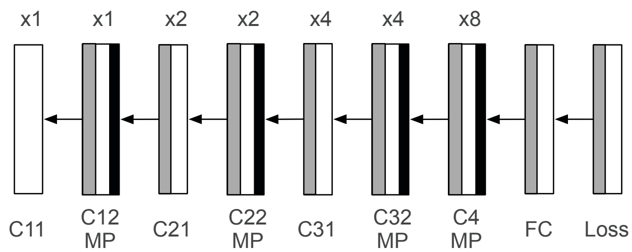

(b) Backward pass of whole network

Fig. 4. Forward and backward pass of whole network (C-Convolution, MP-Max Pooling, FC-Fully Connected, S-Same Padding, V-Valid Padding)

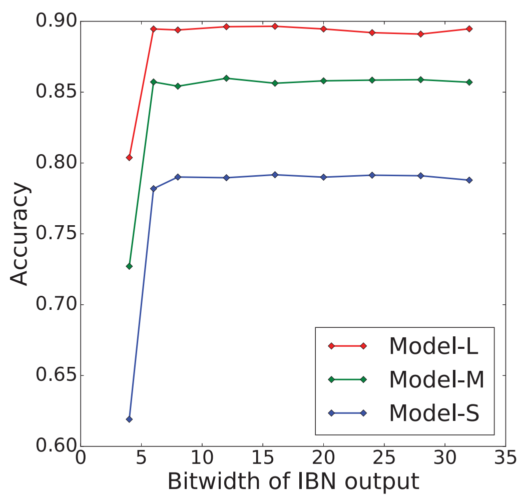

Fig. 5. Accuracy of different BN schemes. Standard BN corresponds to rightmost point (32-bit) and the remaining results denote different bit-width of IBN output (4, 6, 8, 12, 16, 20, 24, 28, 32-bits from left to right).

parameters is sufficient for maintaining performance, and bit-width lower than 8-bits will bring significant accuracy loss. We can also conclude that the adaptive update of scaling factor (Algorithm 1) can fit the value drift and keep values in normal range. On the contrary, static scaling factor imposes too strong regularization on model parameters and fails to converge when bit-width lower than 8-bit. The hyper-parameter setting is identical with Session III-A.

C. Effects of Gradients Bit-width

It has been shown from Figure 1 that gradients are more unstable than primal parameters, which indicates that we

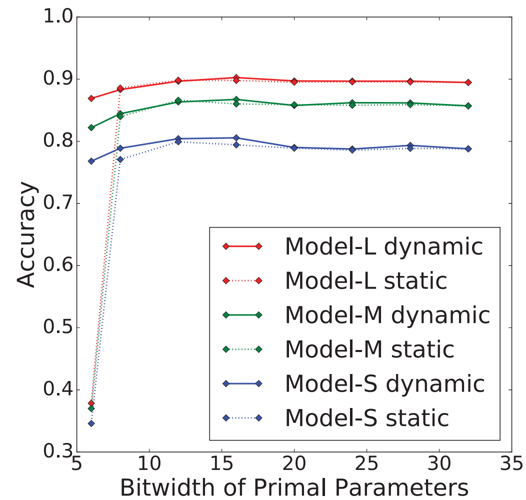

Fig. 6. Accuracy of different bit-width of primal parameters. Gradients are with floating-point values. X-axis denotes different bit-width of primal parameters (6, 8, 12, 16, 20, 24, 28, 32-bits from left to right).

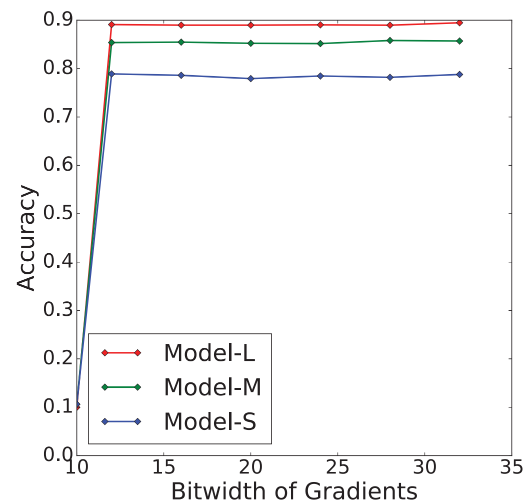

Fig. 7. Accuracy of different gradient bit-widths. Parameters are with floating-point values. X-axis denotes the bit-width (8, 10, 12, 16, 20, 24, 28, 32-bits from left to right).

should update the scaling factors for gradients more frequently. In our experiments, we update it every 375 iterations (1% of total iterations) and use the FxpADAM method. Primal parameters have floating-point values. The results are shown in Figure 7.

We can see that when we reduce the bit-width of gradients, the prediction accuracy also degrades slowly. It then suffers a cliff-off drop when the bit-width is lower than 12 bits for Model-S, Model-M and Model-L. We have observed similar phenomena in Session III-A and Session III-B. All these results indicate that the whole training procedure is likely to be suddenly stuck when the bit-width of any component among IBN output, primal parameters and corresponding gradients is less than a threshold.

TABLE III
PERFORMANCE OF DIFFERENT METHODS

Method	Primal[1] Weight	Running[1] Weight	Activation[1]	Gradient[1]	#Paramter	Inference Relative Complexity [2]	Training Relative Storage [3]	CIFAR-10 Err. Rate
Courbariaux et al. [18]	12	10	10	10	2.88M	100	0.3	14.82%
Miyashita et al. [19]	32	5	4	5	14.02M	20	4.0	6.21%
BCN (det.) [20]	32	1	32	32	14.02M	32	4.0	9.90%
BNN, QNN (Theano) [22], [25]	32	1	1	32	14.02M	1	4.0	11.40%
FxpNet[4] (Model-L)	24	1	1	24	9.29M	1	2.0	10.30%
	16	1	1	16	9.29M	1	1.3	10.51%
	12	1	1	12	9.29M	1	1.0	11.48%

[1] Bit-width of these primal weight, running weight, activation and gradient
[2] Inference Relative Complexity $=$ Running Weight $\times$ Activation
[3] Training Relative Storage $=$ #Parameter $\times$ Primal Weight
[4] Bit-width of IBN output is 12-bit

D. Combining All Components

We further investigate the effects by combining quantization of IBN output, primal parameters and corresponding gradients. Table III summarizes these results and compares them with the state-of-art works. It is shown that FxpNet has managed to push the boundary of model quantization and binarization with 12-bit primal weights and 12-bits gradient, achieving comparable result with state-of-the-art works on the CIFAR-10 dataset. Compared with BNN [22], FxpNet consume one quarter of storage capacity and much less training complexity [1] to achieve similar prediction accuracy on CIFAR-10 dataset. FxpNet proves that linear quantization on gradients works well on networks with binarized weights and activations. It should be noted that although Miyashita et al. [19] achieve a fairly low error rate with 6.21%, their network is more complicated and they do not constrain the running weights and activation to binary values, which results in much higher inference complexity.

IV. RELATED WORK

Model quantization was first fully investigated in CNNs during the training stage in [18] where 10-bit multiplications are sufficient for training Maxout networks. Miyashita et al. [19] proposed a logarithmic representation to quantize weights, activations and gradients, finding that logarithmic quantization is better than linear linear quantization method and the 5-bits logarithmic representation reserves comparable accuracy over the CIFAR-10 dataset. Vanhoucke et al. [8] store activations and weights with 8-bit values, but they only apply this process to trained neural networks without retraining the model. Courbariaux et.al. [20] first introduce model binarization and propose the BinaryConnect algorithm (BCN) to achieve near state-of-art performance on PI-MNIST, CIFAR-10 and SVHN datasets. Lin et al. [21] continue this work and convert the multiplications to bit-shift during back propagation. BNN [22] extends BCN and successfully binarizes both weights and activations without accuracy degradation in aforementioned datasets. At almost the same time, Rastegari et al. [23] propose XNOR-Net and evaluate it on the more challenging ImageNet dataset. Later on Zhou et al. [24] propose DoReFa-Net, further quantizing the gradients and obtaining about 46.1% top-1 accuracy on the ImageNet validation set with 1-bit weights, 2-bit activations and 6-bit gradients. More recently, Hubara et al. [25] have proposed QNN, which surpasses DoReFa-Net and has become a the state-of-the-art approach. Table IV lists the comparison of these methods. All gradients and primal parameters are floating point values in BNN [22]. QNN [25] and DoReFa-Net [24] quantize the gradients but still keep the floating-point values for primal parameters. As a comparison, both of them are quantized into fixed-point representations in FxpNet. It is noteworthy that FxpNet still keeps the binarized activations that are in a 2-bits quantized format in QNN and DoReFa-Net.

[1]It is hard to give a quantitative analysis on training complexity.

TABLE IV
COMPARISON AMONG DIFFERENT MODEL QUANTIZATION AND BINARIZATION APPROACHES.

Method	Primal[1] Weight	Running[1] Weight	Activation[1]	Gradient[1]
Courbariaux et al. [18]	12	10	10	10
Miyashita et al. [19]	32	5	4	5
BCN [20]	32	1	32	32
BNN [22]	32	1	1	32
XNOR-Net [23]	32	1	1	32
DoReFa-Net [24]	32	1	2	6
QNN [25]	32	1	2	6

[1] Bit-width of primal weight, running weight, activation and gradient

Related works also exist for accelerating model training and serving. Gong et al. [9] systematically analyze different vector quantization approaches and find that k-mean clustering among weights makes an appropriate tradeoff between compression efficiency and prediction accuracy. Zhang et al. [11] take nonlinear units into consideration and minimize the reconstruction error with low-rank constraints. Han et al. [10] propose a pipeline to compress trained models, including pruning small weights, quantizing the remaining ones and applying Huffman coding.

V. CONCLUSION AND FUTURE WORK

We have introduced FxpNet, a framework to train DCNNs with low bit-width arithmetics in both forward pass and backward pass. In forward pass, FxpNet takes advantage of the fixed-point format to represent primal parameters and binarizes both weights and activations. In backward pass all gradients are represented in fixed-point format. FxpNet manages to achieve the state-of-the-art results, and pushes the limit of model quantization and binarization.

FxpNet introduces IBN and FxpADAM methods to further reduce required floating-point operations. It also goes a step further to provide a pure fixed-point neural network almost without expensive floating-point operations, which is of vital importance for FPGAs and dedicated ASICs implementation.

There are still opportunities for further improvement. One direction is to allocate more bit-width to activations as QNN and DoReFa-Net. This way, the bit-width of primal parameters and gradients would be further reduced. Another direction is to remove the remaining floating-point operations; the $\mathrm{SoftmaxCrossEntropyLoss}$ layer and the gradients within IBN. Combining them together, we believe that FxpNet could achieve good results on more challenging ImageNet dataset.

ACKNOWLEDGMENT

We would like to express our appreciation to Hao Liang, Wenqiang Wang and Fangzhou Liao for their valuable feedback. This work was supported in part by the National Basic Research Program (973 Program) of China under Grant 2013CB329403, in part by the National Natural Science Foundation of China under Grant 91420201, Grant 61332007, and Grant 61621136008, and in part by the German Research Foundation (DFG) under Grant TRR-169.

REFERENCES

[1] A. Krizhevsky, I. Sutskever, and G. E. Hinton, "Imagenet classification with deep convolutional neural networks," in *Advances in neural information processing systems*, 2012, pp. 1097–1105.

[2] C. Szegedy, W. Liu, Y. Jia, P. Sermanet, S. Reed, D. Anguelov, D. Erhan, V. Vanhoucke, and A. Rabinovich, "Going deeper with convolutions," in *Proceedings of the IEEE Conference on Computer Vision and Pattern Recognition*, 2015, pp. 1–9.

[3] J. Devlin, R. Zbib, Z. Huang, T. Lamar, R. M. Schwartz, and J. Makhoul, "Fast and robust neural network joint models for statistical machine translation." in *ACL (1)*. Citeseer, 2014, pp. 1370–1380.

[4] D. Bahdanau, K. Cho, and Y. Bengio, "Neural machine translation by jointly learning to align and translate," *arXiv preprint arXiv:1409.0473*, 2014.

[5] G. Hinton, N. Srivastava, and K. Swersky, "Neural networks for machine learning," *Coursera, video lectures*, vol. 264, 2012.

[6] T. N. Sainath, A.-r. Mohamed, B. Kingsbury, and B. Ramabhadran, "Deep convolutional neural networks for lvcsr," in *2013 IEEE International Conference on Acoustics, Speech and Signal Processing*. IEEE, 2013, pp. 8614–8618.

[7] T. W. D. J. W. A. Y. N. Adam Coates, Brody Huval and B. Catanzaro, "Deep learning with cots hpc systems," in *ICML*, 2013.

[8] V. Vanhoucke, A. Senior, and M. Z. Mao, "Improving the speed of neural networks on cpus," 2011.

[9] Y. Gong, L. Liu, M. Yang, and L. Bourdev, "Compressing deep convolutional networks using vector quantization," *arXiv preprint arXiv:1412.6115*, 2014.

[10] S. Han, H. Mao, and W. J. Dally, "Deep compression: Compressing deep neural networks with pruning, trained quantization and huffman coding," *arXiv preprint arXiv:1510.00149*, 2015.

[11] X. Zhang, J. Zou, X. Ming, K. He, and J. Sun, "Efficient and accurate approximations of nonlinear convolutional networks," in *CVPR*, 2015, pp. 1984–1992.

[12] S. K. Kim, L. C. McAfee, P. L. McMahon, and K. Olukotun, "A highly scalable restricted boltzmann machine fpga implementation," in *2009 International Conference on Field Programmable Logic and Applications*. IEEE, 2009, pp. 367–372.

[13] C. Farabet, B. Martini, B. Corda, P. Akselrod, E. Culurciello, and Y. LeCun, "Neuflow: A runtime reconfigurable dataflow processor for vision," in *CVPR 2011 Workshops*. IEEE, 2011, pp. 109–116.

[14] P.-H. Pham, D. Jelaca, C. Farabet, B. Martini, Y. LeCun, and E. Culurciello, "Neuflow: Dataflow vision processing system-on-a-chip," in *2012 IEEE 55th International Midwest Symposium on Circuits and Systems (MWSCAS)*. IEEE, 2012, pp. 1044–1047.

[15] Y. Chen, T. Luo, S. Liu, S. Zhang, L. He, J. Wang, L. Li, T. Chen, Z. Xu, N. Sun *et al.*, "DaDianNao: A machine-learning supercomputer," in *Proceedings of the 47th Annual IEEE/ACM International Symposium on Microarchitecture*. IEEE Computer Society, 2014, pp. 609–622.

[16] S. Han, X. Liu, H. Mao, J. Pu, A. Pedram, M. A. Horowitz, and W. J. Dally, "Eie: efficient inference engine on compressed deep neural network," *arXiv preprint arXiv:1602.01528*, 2016.

[17] J. Qiu, J. Wang, S. Yao, K. Guo, B. Li, E. Zhou, J. Yu, T. Tang, N. Xu, S. Song *et al.*, "Going deeper with embedded fpga platform for convolutional neural network," in *Proceedings of the 2016 ACM/SIGDA International Symposium on Field-Programmable Gate Arrays*. ACM, 2016, pp. 26–35.

[18] M. Courbariaux, J.-P. David, and Y. Bengio, "Training deep neural networks with low precision multiplications," *arXiv preprint arXiv:1412.7024*, 2014.

[19] D. Miyashita, E. H. Lee, and B. Murmann, "Convolutional neural networks using logarithmic data representation," *arXiv preprint arXiv:1603.01025*, 2016.

[20] M. Courbariaux, Y. Bengio, and J.-P. David, "Binaryconnect: Training deep neural networks with binary weights during propagations," in *Advances in Neural Information Processing Systems*, 2015, pp. 3123–3131.

[21] Z. Lin, M. Courbariaux, R. Memisevic, and Y. Bengio, "Neural networks with few multiplications," *arXiv preprint arXiv:1510.03009*, 2015.

[22] M. Courbariaux and Y. Bengio, "Binarynet: Training deep neural networks with weights and activations constrained to+ 1 or-1," *arXiv preprint arXiv:1602.02830v3*, 2016.

[23] M. Rastegari, V. Ordonez, J. Redmon, and A. Farhadi, "Xnor-net: Imagenet classification using binary convolutional neural networks," *arXiv preprint arXiv:1603.05279*, 2016.

[24] S. Zhou, Y. Wu, Z. Ni, X. Zhou, H. Wen, and Y. Zou, "Dorefa-net: Training low bitwidth convolutional neural networks with low bitwidth gradients," *arXiv preprint arXiv:1606.06160*, 2016.

[25] I. Hubara, M. Courbariaux, D. Soudry, R. El-Yaniv, and Y. Bengio, "Quantized neural networks: Training neural networks with low precision weights and activations," *arXiv preprint arXiv:1609.07061*, 2016.

[26] M. Abadi, A. Agarwal, P. Barham, E. Brevdo, Z. Chen, C. Citro, G. S. Corrado, A. Davis, J. Dean, M. Devin *et al.*, "Tensorflow: Large-scale machine learning on heterogeneous distributed systems," *arXiv preprint arXiv:1603.04467*, 2016.

[27] Y. Bengio, N. Léonard, and A. Courville, "Estimating or propagating gradients through stochastic neurons for conditional computation," *arXiv preprint arXiv:1308.3432*, 2013.

[28] J. L. Holt and T. E. Baker, "Back propagation simulations using limited precision calculations," in *Neural Networks, 1991., IJCNN-91-Seattle International Joint Conference on*, vol. 2. IEEE, 1991, pp. 121–126.

[29] D. Kingma and J. Ba, "Adam: A method for stochastic optimization," *arXiv preprint arXiv:1412.6980*, 2014.

[30] A. Krizhevsky and G. Hinton, "Learning multiple layers of features from tiny images," 2009.

[31] N. Srivastava, G. E. Hinton, A. Krizhevsky, I. Sutskever, and R. Salakhutdinov, "Dropout: a simple way to prevent neural networks from overfitting." *Journal of Machine Learning Research*, vol. 15, no. 1, pp. 1929–1958, 2014.